Iron inhibits hydroxyapatite crystal growth in vitro

Pascal Guggenbuhl, Robert Filmon, Guillaume Mabilleau, Michel-Félix Baslé, Daniel Chappard

Available online at www.sciencedirect.com
ScienceDirect
Acta Biomaterialia 4 (2008) 1762–1769
Acta BIOMATERIALIA
www.elsevier.com/locate/actabiomat

Chemical structure of methylmethacrylate-2-[2′,3′,5′-triiodobenzoyl] oxoethyl methacrylate copolymer, radio-opacity, in vitro and in vivo biocompatibility

Catalin Zaharia [a,b], Teodora Zecheru [a,b], Marie Françoise Moreau [b], Florence Pascaretti-Grizon [b], Guillaume Mabilleau [b], Bogdan Marculescu [a], Robert Filmon [b], Corneliu Cincu [a,b], Georges Staikos [c], Daniel Chappard [b,*]

[a] Department of Macromolecular Compounds, Faculty of Applied Chemistry and Materials Science, University POLITEHNICA, Bucharest 010072, Romania
[b] INSERM, U922-LHEA, Faculté de Médecine, Angers Cedex 49045, France
[c] Faculty of Chemical Engineering, University of Patras, Greece

Received 18 February 2008; received in revised form 27 May 2008; accepted 18 June 2008
Available online 2 July 2008

Abstract

The properties of copolymers (physical, chemical, biocompatibility, etc.) depend on their chemical structure and microstructural characteristics. We have prepared radio-opaque polymers based on the copolymers of methyl methacrylate (MMA) and 2-[2′,3′,5′-triiodobenzoyl]oxoethyl methacrylate (TIBOM). The copolymerization reaction between TIBOM and MMA showed that the reactivity ratios were $r_1 = 0.00029$ and $r_2 = 1.2146$. The composition diagram is typical for a practically non-homopolymerizable monomer (TIBOM) and a very reactive monomer (MMA). The copolymers were analyzed on an X-ray microcomputed tomograph and they proved to be radio-opaque even at low concentrations of TIBOM. The biocompatibility was tested both in vitro (with J774.2 macrophage and SaOS-2 osteoblast like cells) and in vivo in the rat. These materials were found to be non-toxic and were well tolerated by the organism. These combined results led to the suggestion that this type of polymer could be used as dental or bone cements in place of barium or zirconium particles, which are usually added to provide X-ray opacity.

Keywords: Iodine-containing polymers; pMMA; Radio-opacity; MicroCT; Biocompatibility

1. Introduction

Polymeric biomaterials play a major role in the medical field. A plethora of polymeric biomaterials have been developed to meet the requirements with respect to biocompatibility, chemical properties, mechanical resistance, etc. For example, poly(methyl methacrylate) (pMMA) is used as dental and bone cement, different acrylates are used in ophthalmology and poly(urethanes) are applied for the manufacture of catheters [1–6]. A major drawback of polymeric biomaterials is that they are radiolucent, since polymers hardly absorb X-ray radiation due to the absence of heavy elements within their structure. When a biomaterial is used inside the body (temporarily or permanently), it is often necessary to visualize it through X-ray radiation. One well-known solution, especially in the case of dental and bone cements, is the incorporation of inorganic additives, such as barium sulphate or zirconium dioxide particles. In the case of methacrylic bone cements, it has been reported that these particles diminish the mechanical properties (especially fatigue life) due to the creation of interfaces between the polymeric matrix and the inorganic radio-opacifying particles [1, 7–12]. In addition, the release of such particles has been found to be deleterious to bone since they activate bone resorption [13].

* Corresponding author. Tel.: +33 241 73 5864; fax: +33 241 73 5886.
E-mail address: daniel.chappard@univ-angers.fr (D. Chappard).

1742-7061/$ - see front matter © 2008 Acta Materialia Inc. Published by Elsevier Ltd. All rights reserved.
doi:10.1016/j.actbio.2008.06.009

An ideal solution would be to obtain a homogeneous polymer containing specific groups that confer radio-opacity to the material. Several authors have proposed the use of copolymers containing monomers with covalently bound iodine, which ensure radio-opacity, in the preparation of radio-opaque cements or embolization beads [14–21]. Iodine is known to be radio-opaque due to its high atomic weight (relative atomic mass = 127). In this respect, we synthesized several copolymers composed of methyl methacrylate (MMA) and an iodine-based monomer, namely 2-[2′,3′,5′-triiodobenzoyl]oxoethyl methacrylate (TIBOM). These copolymers exhibit intrinsic X-ray visibility in combination with in vitro cell compatibility and good in vivo tissue compatibility. TIBOM is a convenient iodine-based monomer as it is easily prepared and purified, and its copolymerization with MMA is achieved with very good yields. We were also interested in the microstructural details (i.e. the distribution of the monomer units along the macromolecular chain) of the copolymers, and the reactivity ratios of the two monomers were determined by the most common integral and differential equations. The cytocompatibility of the polymers was determined by an in vitro assay with macrophages and osteoblast-like cells. Finally, the polymer was implanted subcutaneously into rats and it proved to be well tolerated in a long-term experiment.

2. Materials and methods

2.1. Polymer preparation

MMA (Merck) was used after a preliminary purification by distillation in vacuo (63 °C and 200 mmHg). The iodine-containing monomer TIBOM was prepared in pure form. 2-Hydroxyethyl methacrylate (HEMA) (Fluka) was distilled under reduced pressure (45 °C, 2.1×10^{-3} bar) and stored at −20 °C. Ethylene glycol dimethacrylate (EGDMA) (Aldrich) was used as supplied without any further purification. Benzoyl peroxide (BPO) (Merck) was employed, and was purified through recrystallization from methanol at 40 °C. Toluene (S.C. Reagent) was distilled (110 °C, 1 bar pressure) and stored at +8 °C. Dichloromethane and triethylamine (TEA) were purchased from Aldrich and used without purification. Tetrahydrofuran (THF, Merck) was purified by distillation in the following manner: first, it was distilled on cuprous chloride ($CuCl_2$), then the medium fraction was deposited on potassium hydroxide pellet (KOH) overnight and finally it was rectified over metallic sodium (66.8 °C).

2.2. Synthesis of TIBOM

(Fig. 1) At room temperature, thionyl chloride (19 g, 159.7 mmol) was added dropwise to a magnetically stirred solution of 2,3,5-triiodobenzoic acid (40 g, 80.13 mmol) in 300 ml of anhydrous THF. Because the reaction produces potentially dangerous by-products, it was performed in a fume hood under inert atmosphere. The gaseous effluents were passed through a retention turn filled with Natron asbestos. The residual tetrahydrofuran and $SOCl_2$ were evacuated by rotoevaporation. After completion of the addition the reaction mass was refluxed for 30 min, and then allowed to cool at room temperature. The residue 2,3,5-triiodobenzoyl chloride was dissolved in 450 ml of anhydrous dichloromethane. The solution was magnetically stirred and cooled to −5 °C and a solution of HEMA (11.47 g, 88.14 mmol) and TEA (32.43 g, 320.52 mmol) in 50 ml of anhydrous dichloromethane was added dropwise. After the addition was completed, the ice bath was removed and stirring was continued for 1 h at room temperature. The reaction mixture was then cooled again at −5 °C and water (~150 ml) was carefully added. The reaction mass was transferred to a separator funnel and the organic layer was separated. The organic layer was washed with 0.1 M $NaHCO_3$ solution (once) and brine (twice), dried over magnesium sulphate ($MgSO_4$), filtered and concentrated. The crude product was recrystallized from a mixture of hexane and ethanol as a white-brownish powder (77% yield, mp = 99.5 °C). Proton nuclear magnetic resonance was used to control the identity and purity of the TIBOM monomer (spectrum not shown).

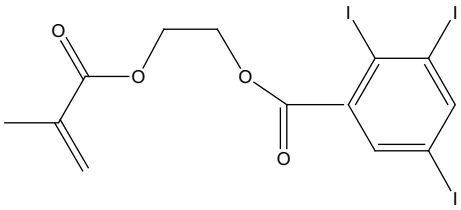

Fig. 1. Molecular structure of TIBOM.

2.3. Preparation of MMA–TIBOM copolymers

Copolymers were prepared in solution for performing the kinetic study and in bulk for preparing cylinders that can be used for in vitro and in vivo experiments.

Copolymerization in a MMA–TIBOM solution was done by increasing the concentration of TIBOM monomer (0.1, 0.2, 0.3, 0.4, and 0.5 molar fraction). For each composition we prepared three samples with equal volumes, which were polymerized for 30, 50, and 90 min starting from the appearance of the first copolymer particle. The reaction was carried out in the presence of benzoyl peroxide (5×10^{-3} mol l^{-1}) as initiator and toluene as solvent. The copolymerization was performed at 75 °C under a nitrogen atmosphere. The copolymers obtained were precipitated in ethylic ether, dried at 40 °C and purified by repeated washing with ethylic ether.

For bulk copolymerization, the monomers, initiator ([BPO] = 10^{-2} mol per mol of monomers) and the cross-linking agent EGDMA (3% molar with respect to monomers mixture) were mixed together by vortexing at 30 Hz, then poured into polyethylene moulds (10 mm in diameter

and 3 mm in height). Polymerizations were carried out in inert atmosphere, at 75 °C for 5 h, followed by post-polymerization at 110 °C, for 3 h. The obtained pellets were immersed in ethanol for 2 days to extract the residual monomers.

A series of MMA–TIBOM copolymers were synthesized as rods (2 mm in diameter) with increasing concentrations of TIBOM (3, 5, 9.5, 14.75, 17, 20.9, 23.1, and 28.6% gravimetric fraction). The reactions were carried out in polyethylene ampoules with BPO as the initiator, at 75 °C under inert atmosphere, for 8 h. The polymers were extracted with ethanol for 2 days to remove the residual monomers

2.4. Characterization techniques of the copolymers

The molecular weights of the copolymers were evaluated by gel permeation chromatography (GPC) analysis. This analysis was done on an HPLC waters 510 chromatograph with styragel tetrahydrofuran columns. This analysis was necessary as all the kinetic models of binary copolymerization are valid only for polymers with a sufficiently high molecular weight.

Raman analysis was performed on a Senterra microscope with the OPUS 5.5 software (BRUKER OPTIK, Ettlingen, Germany). The excitation laser wavelength was 785 nm. The long working distance of the 20× microscope objective gave a spot size in the order of a few micrometers. The Raman microspectroscope consists in a continuous laser beam focused on a sample through a microscope. The pMMA spectrum was compared with the pMMA–TIBOM spectrum.

A kinetic study of the copolymerization reactions were performed with different concentrations and conversion conditions (Table 1). Copolymers were subjected to elemental analysis using a C, H, N analyzer EAGER 200, Stripchart (CE Elantech, Inc., Lakewood, USA). The estimation of the reactivity ratios was done to evaluate the repartition of the different units in the copolymers. For the determination of the reactivity ratios r_1 and r_2, the Mayo–Lewis (ML) equation was assumed to describe better the polymerization process. Several methods were proposed: Finneman–Ross (FR), Kelen–Tüdõs (KT), Tidwell–Mortimer (TM), Yezrielev–Brokhina–Roskin (YBR) and the optimization method OptPex2c [22]. Different reactivity ratios were computed according to the type of method used and all the computations were carried out using the PROCOP computation program [23]. The search of the most probable reactivity ratios through the minimization of F value can be made by OptPex2c method. Using OptPex2c, the instantaneous monomer feed composition M_i, after integration up to the experimental conversion, yielded the cumulative copolymer composition. This composition was compared with the experimentally determined value $m_i^{\exp}$.

2.5. Measurement of X-ray radio-opacity of the copolymers

The X-ray opacity of the samples was measured on two-dimensional (2D) sections of cylinders examined with an X-ray microtomograph (Skyscan 1072, Skyscan Kontich, Belgium). MMA–TIBOM copolymers were fixed on a brass stub with plasticine and a piece of human trabecular was used as control. All specimens were scanned together at 80 kV, 100 μA, 0.9° rotation. The 2D sections were obtained after reconstruction from the projection images obtained in the cone beam mode. On each 2D section, coded on 8 bits, different polymer cylinders were shown in cross-section. Five sections (separated by 200 μm) were transferred to Photoshop CS (Adobe Inc software) and the mean grey level of each polymer sample was determined. The X-ray absorbance was determined as $A = 255$-grey level and ranged from 0 (no X-ray absorption) to 255 (100% absorption), expressed in arbitrary units.

2.6. Cytocompatibility using in vitro culture

Because bone cements are placed in direct contact with bone cells (i.e. osteoblasts and osteoclasts), we investigated the cytocompatibility of the materials on

Table 1
Feed and copolymer composition

Monomer feed molar composition		Conversion (%)	Elemental analysis		Global molar ratio in copolymer	
M_{TIBOM}	M_{MMA}		C (%)	H (%)	gm_{TIBOM}	gm_{MMA}
0.1	0.9	18.08	45.92	5.45	0.0789	0.9211
0.1	0.9	33.55	46.19	5.66	0.0806	0.9194
0.1	0.9	48.46	47.05	5.65	0.0824	0.9176
0.2	0.8	19.27	40.11	3.96	0.1495	0.8505
0.2	0.8	28.42	40.34	3.73	0.1515	0.8485
0.3	0.7	28.15	39.47	4.21	0.2156	0.7844
0.3	0.7	46.58	39.82	3.62	0.2230	0.7770
0.3	0.7	54.78	38.58	3.44	0.2270	0.7730
0.4	0.6	34.21	34.66	2.61	0.2763	0.7237
0.4	0.6	51.84	35.59	2.48	0.2866	0.7134
0.4	0.6	67.65	35.60	2.64	0.2990	0.7010
0.5	0.5	42.87	35.36	2.46	0.3351	0.6649
0.5	0.5	54.72	33.25	2.26	0.3444	0.6556
0.5	0.5	81.06	36.17	3.49	0.3839	0.6161

two cell lines: the murine macrophage cell line J774.2 (European Collection of Cell Culture, Salisbury, Wiltshire, England), which is able to express typical osteoclast enzymes when activated [24] and can be used to study the effect of anti-osteoclast drugs [25]; and the SaOS-2 osteoblast-like cell line, which is also often used in biomaterial studies. J774.2 and SaOS-2 cells were cultured on disks composed of either pure pMMA or the copolymer pMMA–TIBOM containing 10% of the iodinated monomer. Controls were obtained in 24-well plates composed of standard uncoated polystyrene (Costar, Cambridge, MA) with Dulbecco's modified Eagle's medium (DMEM; Eurobio, Les Ulis, France) containing 10% fetal calf serum (Seromed; Strasbourg, France) and 100 UI ml^{-1} of penicillin and 100 μg ml^{-1} of streptomycin (Eurobio) at 37 °C in a humidified incubator with 5% CO_2.

Cells were cultured on disks composed of either pure pMMA or the copolymer pMMA–TIBOM containing 10% of the iodinated monomer. Each disk was washed 2 h in phosphate-buffered saline (PBS) on a rolling platform, air-dried and sterilized by 6 h under ultraviolet radiation. Controls were obtained on cells grown directly onto the well surface. All experiments were done at least in triplicate; results are provided as means ± standard error of the mean.

For cytotoxicity assays, 105 cells in 50 μl of culture medium were seeded onto polymer disks and the control surface for 2 h to allow cell attachment. In each well, 1 ml of culture medium was added for 3 days. The MTT assay (3-(4,5-dimethylthiazol-2-yl)-2,5-diphenyl tetrazolium bromide; Sigma, France) was used to test the cell viability [26]. A 100 μl volume of MTT stock solution (5 mg ml^{-1} in PBS) was added to each well. For each experiment, a blank medium (without cell) was included. The cells were incubated for 2 h at 37 °C in a CO_2 incubator to allow the yellow dye to be transformed into blue formazan crystals by the mitochondrial dehydrogenase. After incubation, the cells were washed twice with PBS. The insoluble product was dissolved by the addition of 1 ml of acidified 2-propanol (0.04 N HCl in 2-propanol) and mixed to dissolve the dye crystals. The supernatant was removed and centrifuged, and the absorbance was read within 10 nm on a UV-1605 Shimadzu spectrophotometer at a 570 nm wavelength. The optical density is known to reflect the number of living cells.

For electron microscopy, polymer disks were rinsed in PBS buffer, fixed in glutaraldehyde (2.5% in PBS buffer) for 2 h and rinsed three times in PBS buffer. Disks were post-fixed in osmium tetroxide (1% in PBS) for 20 min and rapidly rinsed in distilled water. They were dehydrated in two 2-propanol baths for 2 h, then two 2-propanol/hexamethyldisilazane mixture baths for 10 min. This solvent was evaporated overnight. Disks were carbon coated (10 nm thick) with a MED 020 modular high vacuum coating system (Bal-Tec, Balzers, Liechtenstein) and examined with a JEOL 6301 F field emission scanning electron microscope (JEOL, Paris, France) with an accelerating 5 kV voltage.

2.7. Biocompatibility after in vivo implantation

The research was approved by the University Animal Care Committee. We used six Wistar rats (18- to 19-weeks-old, from Charles River, Cléon, France, average weight 300 ± 52 g), conditioned in a vivarium for 2 weeks (24 °C and 12 h/12 h light/dark cycles). Before surgery, general anesthesia was induced by ketamine (100 mg kg^{-1}) and xylazine (10 mg kg^{-1}). Trichotomy in the dorsal region of each rat and asepsis with chlorhexidine were followed by a linear incision in the skin. Surgical pouches were created in subcutaneous tissue,

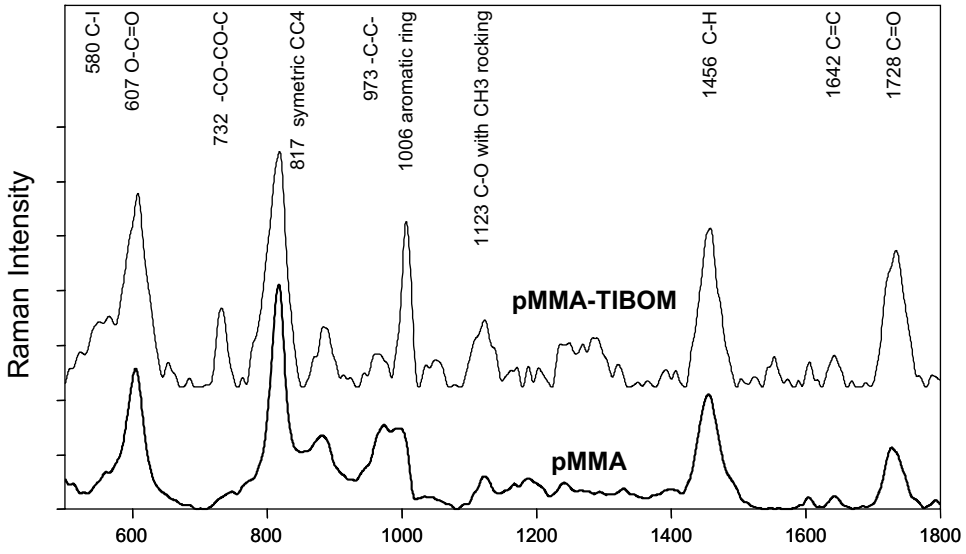

Fig. 2. Raman spectra of pMMA and pMMA–TIBOM. The various peaks are labeled.

Table 2
Reactivity ratios and F criterion

TIBOM–MMA	FR1	FR2	KT	YBR	TM	OptPex2c
r_1	−0.2105	−0.2197	−0.1992	−0.2011	−0.1086	0.00029
r_2	0.8992	0.9018	0.9117	0.9082	0.9830	1.2146
$F \times 10^3$	–	–	–	–	–	43.11

where the capsules were then implanted with a cylinder of the materials. The animals received a normal diet consisting of granular food (UAR, Villemoison sur Orge, France) and water ad libitum and were sacrificed after 120 days. Samples were immediately removed, fixed by immersion in 10% buffered formalin for 24 h, dehydrated in ethanol, clarified in xylene and embedded in paraffin. Histological sections (5 μm thick) were obtained and stained by hematoxylin–phloxine (HE). The intensity of inflammatory infiltrate and fibrosis around the implant cylinders were analyzed by light microscopy.

2.8. Statistical analysis

Statistical study was performed using SYSTAT Release 11 (Systat Software, Inc., San Jose, CA). Data were expressed as means ± standard deviation. Correlations between the mean grey level on microcomputed tomography (microCT) images and TIBOM concentration was searched using linear regression analysis and determination of Pearson's r^2 coefficient. Significant differences between groups were assessed by a non-parametric analysis of variance (Kruskal–Wallis test) with Mann–Whitney's U-test for pairwise comparisons. Differences were considered significant at $p < 0.05$.

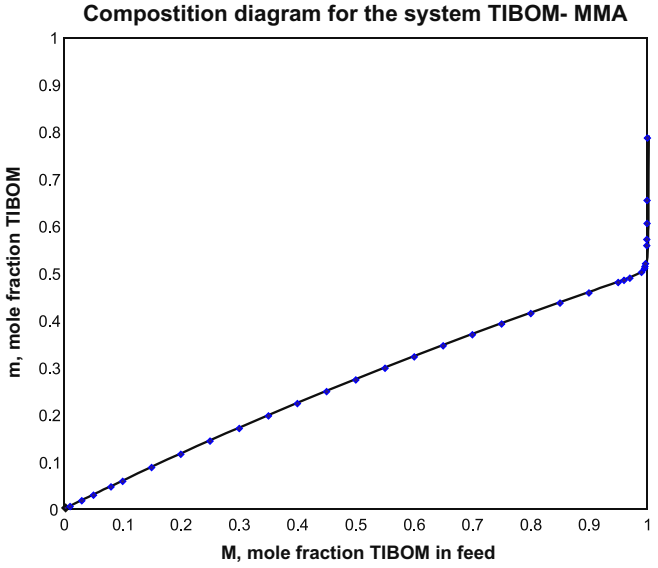

Fig. 3. Mole fraction of TIBOM in TIBOM–MMA copolymer against TIBOM in the substrate ($r_1 = 0.00029$ and $r_2 = 1.2146$).

3. Results and discussion

3.1. Characterization of the copolymers

The GPC analysis showed that the obtained copolymers had molecular weights between 104 and 105 g mol^{-1}. Because of this, all the kinetic models used in the study could be applied with a good precision.

Comparison of the Raman spectra of pMMA and the copolymer MMA–TIBOM confirmed the presence of common bands (O—C=O at 607 cm^{-1}, symmetric CC at 817 cm^{-1}, CH at 1456 cm^{-1} and C=O at 1728 cm^{-1}). Specific bands related to the iodine-linked carbon at 580 cm^{-1}

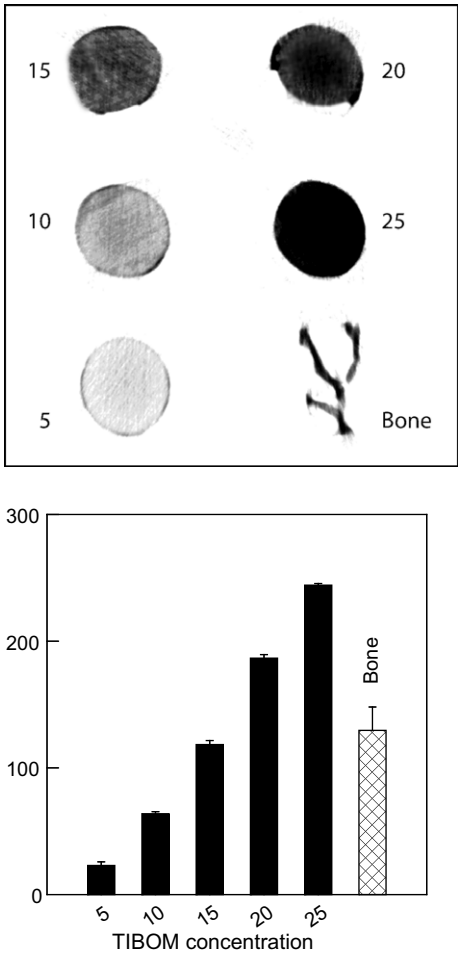

Fig. 4. X-ray opacities. The upper image shows the cylinders of the copolymer TIBOM–MMA in cross-section. The graph illustrates the mean absorbance of X-ray in function of the TIBOM concentration. A ~15% TIBOM concentration in MMA provides a copolymer with the same X-ray opacity as bone matrix.

and the presence of an aromatic ring at 1006 cm^{-1} were evidenced in the TIBOM-containing copolymer (Fig. 2).

The elemental analysis determines the composition of an element with an accuracy lower than 0.2%; therefore it is preferred to the other chemical analyses, which are less accurate. The results presented in Table 1 were used to determine the reactivity ratios for the system MMA–TIBOM. The iodine-containing monomer was less reactive than MMA and the diagram aspect was typically for a system composed of a hardly homopolymerizable monomer (TIBOM) and a very reactive co-monomer (MMA). For the MMA–TIBOM pair the reactivity ratios computed with FR, KT, TD and YBR had no physical meaning (Table 2). Reliable results were, however, obtained by the OptPex2c method (presenting the lowest value for F): $r_1 = 0.00029$ and $r_2 = 1.2146$. The higher r_2 value of MMA shows that this monomer has a higher reactivity than TIBOM. The relationship between the molar fraction of TIBOM in the copolymer MMA–TIBOM and the composition of the substrate is shown in Fig. 3. This composition diagram is typical for a practically non-homopolymerizable monomer (TIBOM) and a very reactive monomer (MMA). This aspect is not surprising, since TIBOM hardly homopolymerizes at all. Nevertheless it does polymerizes, as shown by the value of its reactivity ratio, which is not 0. Taken together, these results suggest that the copolymer is formed by blocks of pMMA intercalated by some units of TIBOM. Several authors have tried other iodinated acrylic monomers to increase radio-opacity, specifically 2-[4-iodobenzoyl]-oxo-ethylmethacrylate [17], 2,5-diiodo-8-quinolyl methacrylate [15] and 3,5-diiodine salicylic methacrylate [9], and also the addition of iodinated molecules dissolved in the cement, such as odixanol, iohexol and iohexol acetate [16]. The radio-opacity obtained with TIBOM is obtained with a smaller amount of monomer since it contains three atoms of iodine.

3.2. MicroCT analysis

MicroCT is a powerful tool in the evaluation of bone and bone biomaterials [27]. All cylinders were scanned together in a single pass so that the grey levels can be measured and compared. The method is more suitable than a projection X-ray film since the heterogeneity within the object composition can be examined. In Fig. 4, MMA–TIBOM copolymers with different fractions of TIBOM are compared with the X-ray opacity of a piece of human trabecular bone. The X-ray opacity of the copolymer MMA–TIBOM increased linearly with TIBOM fraction ($r_2 = 0.99$, $p = 0.00025$). One can see from the graph that a concentration of ~15% in TIBOM within the polymer confer similar radio-opacity than the calcified bone matrix itself.

3.3. Cytocompatibility using cell cultures

The cell types did not differ in terms of morphology and spreading at the surface of pMMA or pMMA–TIBOM (Fig. 5). Numerous cells were encountered at the surface of the polymer disks after 3 days. J774.2 cells were found

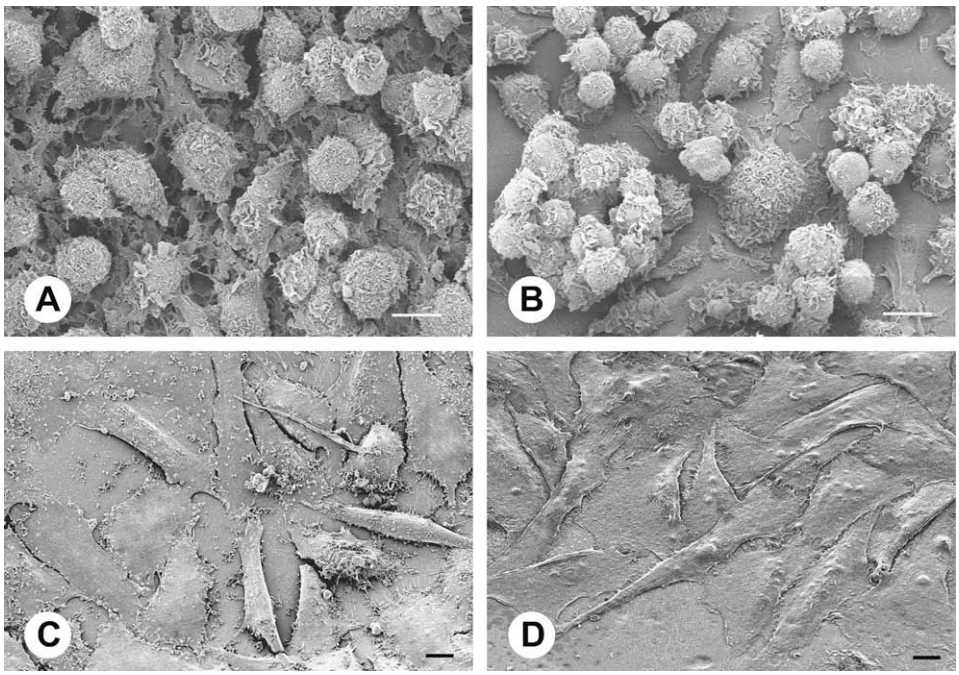

Fig. 5. SEM microphotographs of J774.2 cells (upper micrographs) and SaOS-2 (lower micrographs) cultured on polymer disks composed of pMMA (A and C) or pMMA–TIBOM (B and D). The cells have retained their characteristic appearance with cytoplasm processes and do not exhibit necrotic or apoptotic changes.

mainly to have a round shape, but sometimes exhibited an elongated shape. They exhibited numerous thin filopodia, allowing anchorage to the disks, and sometimes thicker extensions were encountered, allowing communication with cells. SaOS-2 cells appeared flattened and spread onto the surface of both types of polymers. No cytological differences could be seen, and no necrotic cells could be seen at the surface of the polymer disks. The results of the MTT evaluation are provided on Fig. 6. No difference could be observed between the pMMA and pMMA–TIBOM disks; the results differed markedly from the control cells grown on a control surface that had been specially treated to favour cell attachment.

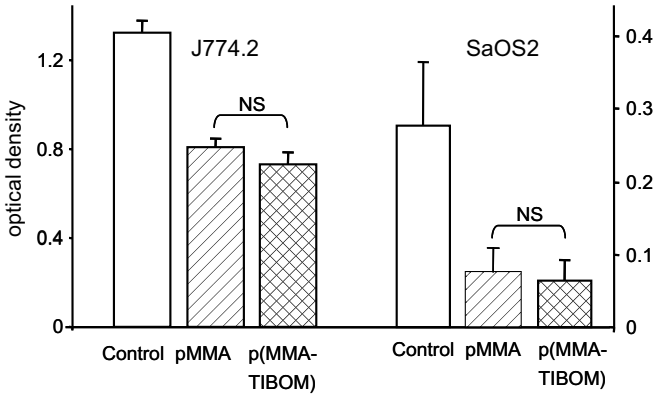

Fig. 6. Results of MTT in J774.2 and SaOS-2 cells. Effects of pMMA and pMMA–TIBOM on MTT reduction compared with cells grown onto a control surface after a 3 days contact.

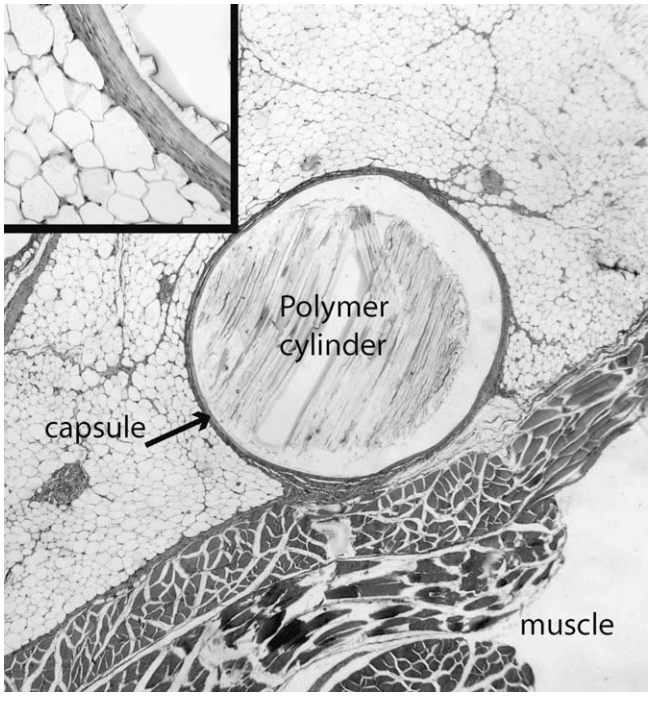

Fig. 7. Biocompatibility testing of pMMA–TIBOM implanted subcutaneously in the rat. Note the position of the cylinder (dissolved by the histological treatment) and the presence of a thin collagenous and fibroblastic capsule (enlarged view at the top). Original magnifications: 50× and 400×.

3.4. Biocompatibility after in vivo implantation

The polymer cylinders were partially dissolved by the histological technique since pMMA is soluble in xylene. However, the position of the polymer always remained well defined. A thin layer of collagenous fibers with elongated fibroblasts was observed, and the membrane was 15.0 ± 4.9 μm in thickness (Fig. 7). No giant cells could be observed in the capsule, and occasionally mast cells were encountered. In one animal there was a moderate lymphocytic infiltration of the membrane, but this was limited to an area in direct contact with muscle fibers.

4. Conclusion

The use of iodine-based monomer provides a convenient way to prepare polymeric biomaterials that uniquely combine X-ray visibility, cellular non-cytotoxicity and in vivo biocompatibility.

The microstructural architecture of the copolymer (that is, the distribution of the monomer units along the macromolecular chain) also influences the mechanical and biological behavior of the material. Replacement of barium sulphate and zirconium dioxide from the bone or dental cements with biocompatible polymers would improve the mechanical properties of the final cement especially upon ageing, since fatigue microcracks are known to start on these material grains.

Acknowledgements

C.Z. received a grant from the Socrates–Erasmus European community program. P. Gras and J. Roux are thanked for their help with the animal care and handling at SCAHU. This work was partially made possible by grants from Contrat de Plan Etat – Region "Pays de la Loire", the Bioregos program and INSERM.

References

[1] Kruft MA, Benzina A, Blezer R, Koole LH. Studies on radio-opaque polymeric biomaterials with potential applications to endovascular prostheses. Biomaterials 1996;17:1803–12.
[2] Kruft MA, van der Veen FH, Koole LH. In vivo tissue compatibility of two radio-opaque polymeric biomaterials. Biomaterials 1997;18:31–6.
[3] Saralidze K, Aldenhoff YB, Knetsch ML, Koole LH. Injectable polymeric microspheres with X-ray visibility. Preparation, properties, and potential utility as new traceable bulking agents. Biomacromolecules 2003;4:793–8.
[4] Topoleski LD, Ducheyne P, Cuckler JM. A fractographic analysis of in vivo poly(methyl methacrylate) bone cement failure mechanisms. J Biomed Mater Res 1990;24:135–54.
[5] Vazquez B, Deb S, Bonfield W. Optimization of benzoyl peroxide concentration in an experimental bone cement based on poly(methyl methacrylate). J Mater Sci 1997;8:455–60.

[6] Vazquez B, Ginebra MP, Gil FJ, Planell JA, Lopez Bravo A, San Roman J. Radiopaque acrylic cements prepared with a new acrylic derivative of iodo-quinoline. Biomaterials 1999;20:2047–53.
[7] Liu C, Green SM, Watkins ND, Gregg PJ, McCaskie AW. Some failure modes of four clinical bone cements. Proc Inst Mech Eng 2001;215:359–66.
[8] Aldenhof YB, Kruft MA, Pijpers AP, van der Veen FH, Bulstra SK, Kuijer R, Koole LH. Stability of radiopaque iodine-containing biomaterials. Biomaterials 2002;23:881–6.
[9] Artola A, Gurruchaga M, Vazquez B, San Roman J, Goni I. Elimination of barium sulphate from acrylic bone cements. Use of two iodine-containing monomers. Biomaterials 2003;24:4071–80.
[10] Davy KWM, Anseau MR, Odlyha M, Foster GM. X-ray opaque methacrylate polymers for biomedical applications. Polymer Int 1997;43:143–54.
[11] Horak D, Metalova M, Rypacek F. New radiopaque polyHEMA-based hydrogel particles. J Biomed Mater Res 1997;34:183–8.
[12] van Hooy-Corstjens CS, Govaert LE, Spoelstra AB, Bulstra SK, Wetzels GM, Koole LH. Mechanical behaviour of a new acrylic radiopaque iodine-containing bone cement. Biomaterials 2004;25:2657–67.
[13] Sabokbar A, Fujikawa Y, Murray DW, Athanasou NA. Radio-opaque agents in bone cement increase bone resorption. J Bone Joint Surg Br 1997;79:129–34.
[14] Rusen E, Zaharia C, Zecheru T, Marculescu B, Filmon R, Chappard D, Badulescu R, et al. Synthesis and characterisation of core–shell structures for orthopaedic surgery. J Biomech 2007;40:3349–53.
[15] Ginebra MP, Aparicio C, Albuixech L, Fernandez-Barragan E, Gil FJ, Planell JA, Morejon L, et al. Improvement of the mechanical properties of acrylic bone cements by substitution of the radio-opaque agent. J Mater Sci 1999;10:733–7.
[16] Lewis G, van Hooy-Corstjens CS, Bhattaram A, Koole LH. Influence of the radiopacifier in an acrylic bone cement on its mechanical, thermal, and physical properties: barium sulfate-containing cement versus iodine-containing cement. J Biomed Mater Res 2005;73:77–87.
[17] van Hooy-Corstjens CS, Bulstra SK, Knetsch ML, Geusens P, Kuijer R, Koole LH. Biocompatibility of a new radiopaque iodine-containing acrylic bone cement. J Biomed Mater Res B 2007;80:339–44.
[18] Ginebra MP, Albuixech L, Fernandez-Barragan E, Aparicio C, Gil FJ, San RJ, Vazquez B, et al. Mechanical performance of acrylic bone cements containing different radiopacifying agents. Biomaterials 2002;23:1873–82.
[19] Mottu F, Rufenacht DA, Laurent A, Doelker E. Iodine-containing cellulose mixed esters as radiopaque polymers for direct embolization of cerebral aneurysms and arteriovenous malformations. Biomaterials 2002;23:121–31.
[20] Okamura M, Uehara H, Yamanobe T, Komoto T, Hosoi S, Kumazaki T. Synthesis and properties of radiopaque polymer hydrogels: polyion complexes of copolymers of acrylamide derivatives having triiodophenyl and carboxyl groups and *p*-styrene sulfonate and polyallylamine. J Mol Struct 2000;554:35–45.
[21] Okamura M, Yamanobe T, Arai T, Uehara H, Komoto T, Hosoi S, Kumazaki T. Synthesis and properties of radiopaque polymer hydrogels II: copolymers of 2,4,6-triiodophenyl- or *N*-(3-carboxy-2,4,6-triiodophenyl)-acrylamide and *p*-styrene sulfonate. J Mol Struct 2002;602-603:17–28.
[22] Stancu IC, Filmon R, Cincu C, Marculescu B, Zaharia C, Tourmen Y, Baslé MF, et al. Synthesis of methacryloyloxyethyl phosphate copolymers and in vitro calcification capacity. Biomaterials 2004;25:205–13.
[23] Hagiopol C. Copolymerization: toward a systematic approach. New York: Kluwer; 1999.
[24] Mabilleau G, Moreau MF, Filmon R, Baslé MF, Chappard D. Biodegradability of poly(2-hydroxyethyl methacrylate) in the presence of the J774 2 macrophage cell line. Biomaterials 2004;25:5155–62.
[25] Moreau MF, Guillet C, Massin P, Chevalier S, Gascan H, Baslé MF, Chappard D. Comparative effects of five bisphosphonates on apoptosis of macrophage cells in vitro. Biochem Pharmacol 2007;73:718–23.
[26] Mosmann T. Rapid colorimetric assay for cellular growth and survival: application to prolifération and cytotoxicity assays. J Immunol Methods 1983;65:55–63.
[27] Chappard D, Blouin S, Libouban H, Baslé MF, Audran M. Microcomputed tomography for the study of hard tissues and bone biomaterials. Microsc Anal 2005;19:17–9.